A model of the cardiac Na^+/K^+ ATPase: An update of the Terkildsen model

Michael Pan, Peter J. Gawthrop, Joseph Cursons, Kenneth Tran, Edmund J. Crampin

Thursday 5th October, 2017

Abstract

Terkildsen et al. (2007) developed a model of the Na^+/K^+ ATPase in ventricular myocytes to study extracellular potassium accumulation in ischaemia. The model accounts for a wide range of experimental data, but there is no publicly available code to reproduce the figures in their paper. Furthermore, due to errors in their analysis, the model is not thermodynamically consistent as originally claimed. In this paper we update the model by Terkildsen et al. so that it is reproducible and thermodynamically consistent. The updated model was reparameterised, and provides a good fit to experimental measurements describing the dependence of the pumping rate on membrane voltage and metabolite concentrations. Since the updated model is thermodynamically consistent, it is well-suited for incorporation into a whole-cell model of a cardiomyocyte for the purposes of studying energetics. We developed a bond graph version of the model to demonstrate its thermodynamic consistency, and to contribute towards a thermodynamically consistent whole-cell model of a cardiomyocyte. CellML and MATLAB code has been included to enhance reproducibility and reusability of our model.

1 Introduction

In cardiomyocytes, physiological concentrations of Na^+ and K^+ are maintained by Na^+/K^+ ATPases located on their plasma membranes. The Na^+/K^+ ATPase is an electrogenic ion pump that uses energy from ATP hydrolysis to drive the transport of Na^+ and K^+ ions against an electrochemical gradient. Terkildsen et al. (2007) published a model of the Na^+/K^+ ATPase in cardiomyocytes to account for the biophysics and thermodynamics of ion transport, with further details described in Terkildsen (2006). This model was incorporated into a whole-cell model of a cardiomyocyte to investigate the mechanisms of extracellular potassium accumulation during ischaemia (Terkildsen et al., 2007). Terkildsen et al. found that reduced Na^+/K^+ ATPase activity was the dominant mechanism for extracellular potassium accumulation. In this paper, we refer to the Na^+/K^+ ATPase model described in Terkildsen et al. (2007) as the Terkildsen et al. model.

The Na^+/K^+ ATPase model presented in Terkildsen et al. (2007) was based the model by Smith and Crampin (2004), and follows the methods proposed by Smith and Crampin (2004) to incorporate thermodynamic constraints and a lumping scheme to simplify the model. A key advantage of the Terkildsen et al. model over the Smith and Crampin (2004) model is that it was fitted to a wider range of data, which included the dependence of pump current on membrane voltage (Nakao and Gadsby, 1989), extracellular sodium (Nakao and Gadsby, 1989), intracellular sodium (Hansen et al., 2002), extracellular potassium (Nakao and Gadsby, 1989) and MgATP (Friedrich et al., 1996). However, the figures for cycling velocity in the original paper are not reproducible using information supplied in the figure legends (Terkildsen et al., 2007, Fig. 2), and the code used to generate those figures is not publicly available. These reproducibility issues are exacerbated by the use of incorrect equations and numerical values (further described in Section 2) which cause

physical and thermodynamic inconsistencies.

In this paper, we aim to address the reproducibility and physical issues of the Terkildsen et al. model by updating the model so that it is reproducible and thermodynamically consistent. We modified some equations of the model to ensure thermodynamic consistency (Section 2), and refitted the updated model to the same data (Section 3). To verify the physical plausibility of the updated model, we developed a bond graph (Oster et al., 1971; Gawthrop and Crampin, 2014) version of the updated model. We refer readers to Gawthrop and Smith (1996); Borutzky (2010); and Gawthrop and Bevan (2007) for further information on bond graph theory. Due to its thermodynamic consistency, our updated model is well-suited for incorporation into a thermodynamic model of a cardiomyocyte to study cardiac energetics. MATLAB and CellML (Lloyd et al., 2004) code has been provided with this paper for reproducibility.

2 Modifications

The Terkildsen model uses the Post-Albers cycle (Apell, 1989), which is a mechanism by which sodium and potassium ions bind one-by-one on one side of the membrane, and unbind on the other side (Figure 1). The full Post-Albers cycle was simplified using the methods of Smith and Crampin (2004) to reduce computational complexity. First, the faster reactions were assumed to be in rapid equilibrium to reduce the full 15-state model to a four-state model with eight modified rate constants. The entire cycle was then assumed to be in steady state to further reduce the model to a single equation for the cycle flux, with metabolite dependence incorporated in a manner that accounted for thermodynamic constraints. We found three issues while reimplementing the Terkildsen et al. model, and made several modifications to remedy these issues as described below:

Issue 1: The equilibrium constants are inconsistent with the number of binding sites. Typically, the kinetic rate constants for identical binding sites are assumed to be proportional to the number of binding sites available for binding or unbinding (Keener and Sneyd, 2009). Thus we modified the reaction scheme in Terkildsen et al. (2007) to be consistent with this assumption (see red parameters in Figure 1).

Issue 2: Terkildsen et al. (2007) derived a detailed balance constraint which was applied during their fitting procedure. This constraint is an equation that relates the kinetic constants defined in Figure 1:

$$\frac{k_1^+ k_2^+ k_3^+ k_4^+ K^0_{d,\mathrm{Na}_e} (K_{d,\mathrm{Na}_e})^2 (K_{d,\mathrm{K}_i})^2}{k_1^- k_2^- k_3^- k_4^- K^0_{d,\mathrm{Na}_i} (K_{d,\mathrm{Na}_i})^2 (K_{d,\mathrm{K}_e})^2 K_{d,\mathrm{MgATP}}} = \exp\left(-\frac{\Delta G^0_{\mathrm{MgATP}}}{RT}\right) \tag{1}$$

where R is the universal gas constant, T is the absolute temperature, and $\Delta G^0_{\mathrm{MgATP}}$ is the standard free energy of MgATP hydrolysis at pH 0. Terkildsen et al. (2007) start with a standard free energy of -29.6kJ/mol at pH 7, but adjust to a physiological pH rather than pH 0. As a result, substituting the model parameter values into equation (1) results in $\Delta G^0_{\mathrm{MgATP}} = -30.2$kJ/mol, which is inconsistent with the typical standard free energy of 11.9kJ/mol at 311K (Tran et al., 2009; Guynn and Veech, 1973). Since this results in an overall equilibrium constant over 10^7-fold greater than the correct value at a temperature of 310K, we decided to use the correct value of $\Delta G^0_{\mathrm{MgATP}} = 11.9$kJ/mol in the detailed balance constraint.

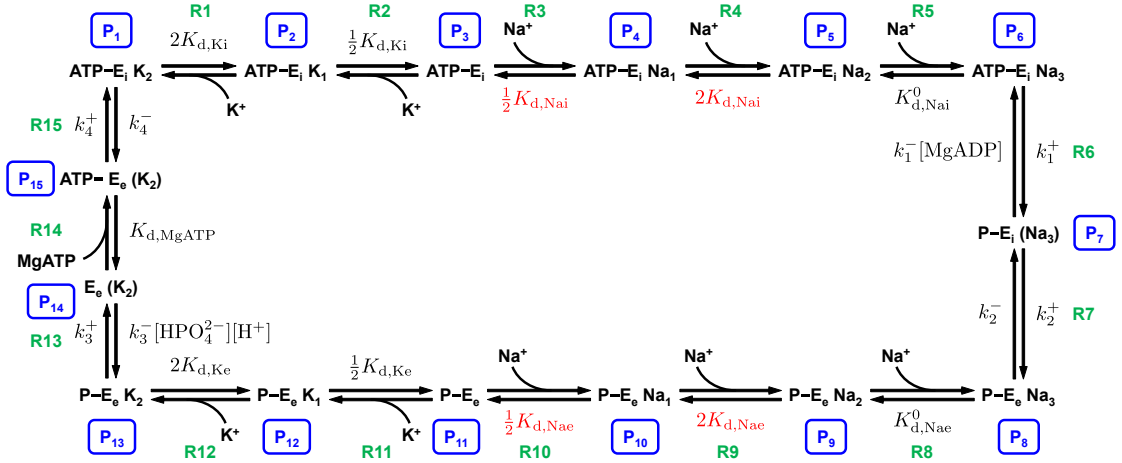

Figure 1: Reaction scheme of the Terkildsen et al. model. The numbers for each pump state are labelled in blue boxes, and reaction names are shown in green. Corrected parameters are coloured in red.

Issue 3: Terkildsen et al. (2007) used a lumping scheme to reduce the 15-state model to a 4-state model with modified kinetic constants. Terkildsen et al. (2007) use similar expressions for the modified rate constants to Smith and Crampin (2004), but those expressions were not applicable to the updated assignment of electrical dependence in Terkildsen et al. (2007). As a result, the expressions for some of the modified rate constants (α_1^+, α_3^+, α_2^- and α_4^-) were incorrect and the original model is an inaccurate representation of pump kinetics. In our updated model, we corrected the equations for these modified rate constants:

$$\alpha_1^+ = \frac{k_1^+ \tilde{\mathrm{Na}}_{i,1} \tilde{\mathrm{Na}}_{i,2}^2}{\tilde{\mathrm{Na}}_{i,1} \tilde{\mathrm{Na}}_{i,2}^2 + (1+\tilde{\mathrm{Na}}_{i,2})^2 + (1+\tilde{\mathrm{K}}_i)^2 - 1} \tag{2}$$

$$\alpha_3^+ = \frac{k_3^+ \tilde{\mathrm{K}}_e^2}{\tilde{\mathrm{Na}}_{e,1} \tilde{\mathrm{Na}}_{e,2}^2 + (1+\tilde{\mathrm{Na}}_{e,2})^2 + (1+\tilde{\mathrm{K}}_e)^2 - 1} \tag{3}$$

$$\alpha_2^- = \frac{k_2^- \tilde{\mathrm{Na}}_{e,1} \tilde{\mathrm{Na}}_{e,2}^2}{\tilde{\mathrm{Na}}_{e,1} \tilde{\mathrm{Na}}_{e,2}^2 + (1+\tilde{\mathrm{Na}}_{e,2})^2 + (1+\tilde{\mathrm{K}}_e)^2 - 1} \tag{4}$$

$$\alpha_4^- = \frac{k_4^- \tilde{\mathrm{K}}_i^2}{\tilde{\mathrm{Na}}_{i,1} \tilde{\mathrm{Na}}_{i,2}^2 + (1+\tilde{\mathrm{Na}}_{i,2})^2 + (1+\tilde{\mathrm{K}}_i)^2 - 1} \tag{5}$$

where

$$\tilde{\mathrm{Na}}_{i,1} = \frac{[\mathrm{Na}^+]_\mathrm{i}}{K^0_{d,\mathrm{Na}_i} e^{\Delta FV/RT}} \qquad \tilde{\mathrm{Na}}_{i,2} = \frac{[\mathrm{Na}^+]_\mathrm{i}}{K_{d,\mathrm{Na}_i}} \tag{6}$$

$$\tilde{\mathrm{Na}}_{e,1} = \frac{[\mathrm{Na}^+]_\mathrm{e}}{K_{d,\mathrm{Na}^0_e} e^{(1+\Delta)zFV/RT}} \qquad \tilde{\mathrm{Na}}_{e,2} = \frac{[\mathrm{Na}^+]_\mathrm{e}}{K_{d,\mathrm{Na}_e}} \tag{7}$$

$$\tilde{\mathrm{K}}_i = \frac{[\mathrm{K}^+]_\mathrm{i}}{K_{d,\mathrm{K}_i}} \qquad \tilde{\mathrm{K}}_e = \frac{[\mathrm{K}^+]_\mathrm{e}}{K_{d,\mathrm{K}_e}} \tag{8}$$

and Δ is the unit of charge translocated by the final sodium binding reaction R5. We derive an expression for α_1^+, and expressions for the other modified rate constants follow

similarly. Since the pump states 1 to 6 are lumped together, the constant k_1^+ is scaled according to the ratio between the amount of state 6 and the total amount of states 1–6. If we represent x_i as the molar amount of state i,

$$\begin{aligned}
\alpha_1^+ &= k_1^+ \frac{x_6}{x_6 + x_5 + x_4 + x_3 + x_2 + x_1} \\
&= k_1^+ \frac{1}{1 + x_5/x_6 + x_4/x_6 + x_3/x_6 + x_2/x_6 + x_1/x_6} \\
&= \frac{k_1^+}{1 + 2\tilde{\mathrm{Na}}_{i,1}^{-1} + 2\tilde{\mathrm{Na}}_{i,1}^{-1}\tilde{\mathrm{Na}}_{i,2}^{-1} + \tilde{\mathrm{Na}}_{i,1}^{-1}\tilde{\mathrm{Na}}_{i,2}^{-2} + 2\tilde{\mathrm{Na}}_{i,1}^{-1}\tilde{\mathrm{Na}}_{i,2}^{-2}\tilde{\mathrm{K}}_i + \tilde{\mathrm{Na}}_{i,1}^{-1}\tilde{\mathrm{Na}}_{i,2}^{-2}\tilde{\mathrm{K}}_i^2} \\
&= \frac{k_1^+ \tilde{\mathrm{Na}}_{i,1}\tilde{\mathrm{Na}}_{i,2}^2}{\tilde{\mathrm{Na}}_{i,1}\tilde{\mathrm{Na}}_{i,2}^2 + (1 + \tilde{\mathrm{Na}}_{i,2})^2 + (1 + \tilde{\mathrm{K}}_i)^2 - 1}
\end{aligned} \tag{9}$$

Because it was not possible to fix the above issues without significantly changing the kinetics of the model, we reparameterised the Terkildsen et al. model such that it would be physically and thermodynamically consistent. In subsequent sections, we shall refer to the reparameterised model with updated equations as the "updated model" and the model with equations and parameters described in (Terkildsen et al., 2007) as the "original model".

3 Reparameterisation of the model

Using the updated model's equations, we fitted parameters to data from Terkildsen et al. (Terkildsen et al., 2007; Terkildsen, 2006). The original model was parameterised by minimising an objective function that measured the divergence of the model from the data. We parameterised the updated model using the methods of Terkildsen (2006), and setting $\Delta G^0_{\mathrm{MgATP}}$ to its correct value of 11.9kJ/mol in the thermodynamic constraint (Equation (1)). Other minor changes to the fitting procedure include:

1. The weighting for extracellular potassium above 5.4 mM for the data of Nakao and Gadsby (1989) was increased from 6× to 15× to obtain a reasonable fit at physiological concentrations.
2. To ensure that the resulting cycling velocities had magnitudes that matched Nakao and Gadsby (1989), the curve for $[\mathrm{Na}]_e = 150\mathrm{mM}$ was fitted in its un-normalised form.
3. Rather than using a local optimiser with literature sources for initial parameter estimates, we used particle swarm optimisation (Kennedy and Eberhart, 1995) followed by a local optimiser to find a global minimum of the objective function.

The results of the fitting process are shown in Figures 2 and 3. The updated model provides good fits to each data source, and the quality of fits are comparable to Terkildsen (2006). Despite a slightly worse fit at lower extracellular sodium concentrations compared to the original model (Figure 2(a)) the unnormalised cycling velocities (Figure 2(b)) appear to be more consistent with experimental data that suggest saturated cycling velocity at positive membrane potentials is relatively insensitive to extracellular sodium (Nakao and Gadsby, 1989). Updated model parameters are given in Table 1 of Appendix A.

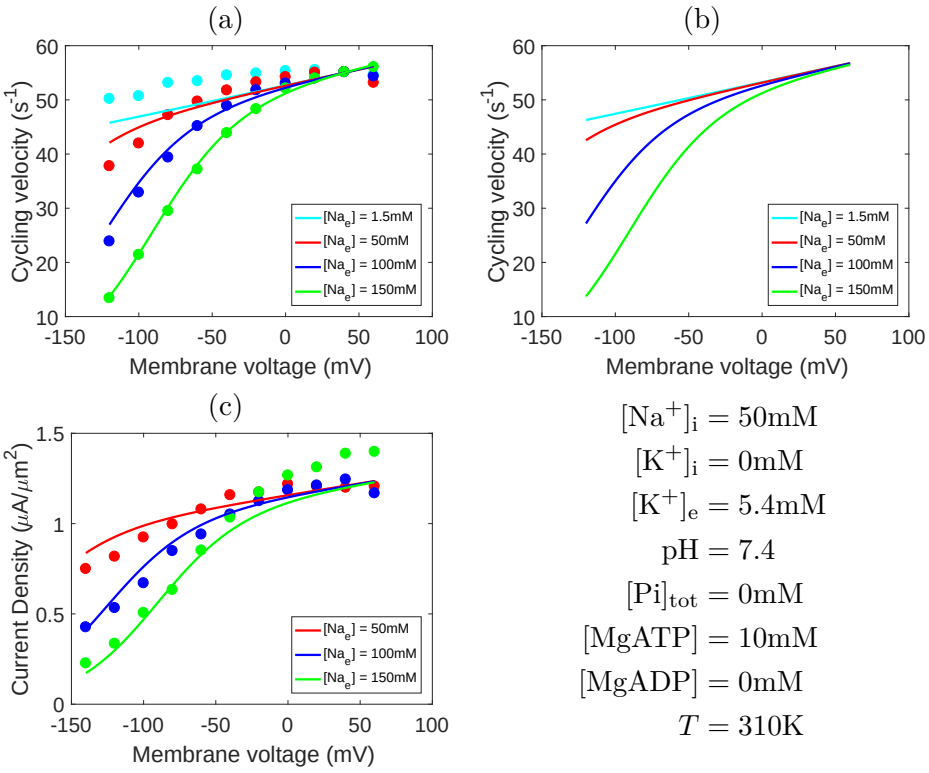

Figure 2: Fit of the updated Terkildsen model to current-voltage measurements. **(a)** Comparison of model to extracellular sodium and voltage data (Nakao and Gadsby, 1989, Fig. 3). Cycling velocities were normalised to a value of $55\mathrm{s}^{-1}$ at $V = 40\mathrm{mV}$. **(b)** Unnormalised cycling velocties. **(c)** Comparison of model to whole-cell current measurements (Nakao and Gadsby, 1989, Fig. 2(a)).

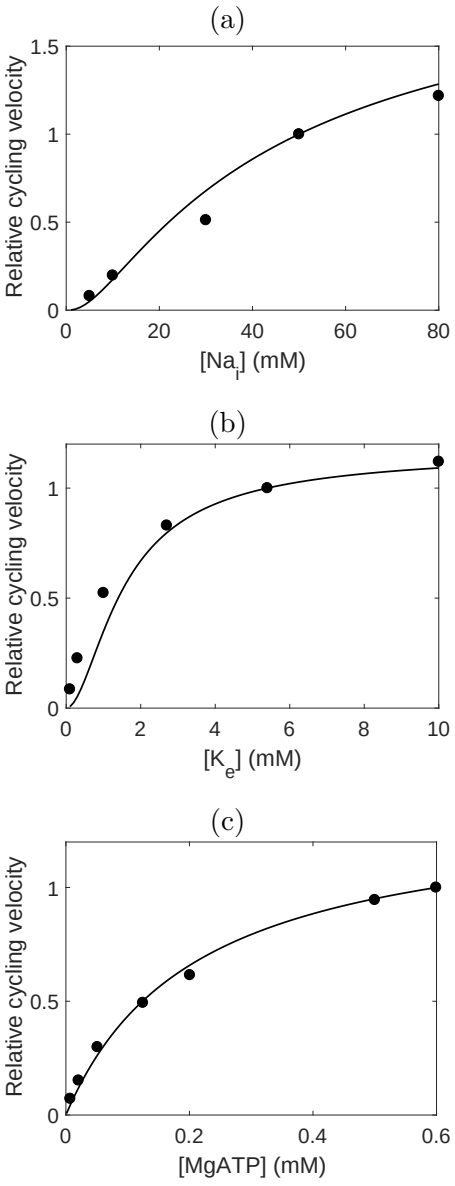

$V = -40\text{mV}$
$[\text{Na}^+]_\text{e} = 140\text{mM}$
$[\text{K}^+]_\text{i} = 70\text{mM}$
$[\text{K}^+]_\text{e} = 5.4\text{mM}$
$\text{pH} = 7.2$
$[\text{Pi}]_\text{tot} = 1\text{mM}$
$[\text{MgATP}] = 2\text{mM}$
$[\text{MgADP}] = 0\text{mM}$
$T = 309\text{K}$

$V = 0\text{mV}$
$[\text{Na}^+]_\text{i} = 50\text{mM}$
$[\text{Na}^+]_\text{e} = 150\text{mM}$
$[\text{K}^+]_\text{i} = 140\text{mM}$
$\text{pH} = 7.4$
$[\text{Pi}]_\text{tot} = 0.5\text{mM}$
$[\text{MgATP}] = 10\text{mM}$
$[\text{MgADP}] = 0.02\text{mM}$
$T = 310\text{K}$

$V = 0\text{mV}$
$[\text{Na}^+]_\text{i} = 40\text{mM}$
$[\text{Na}^+]_\text{e} = 0\text{mM}$
$[\text{K}^+]_\text{i} = 0\text{mM}$
$[\text{K}^+]_\text{e} = 5\text{mM}$
$\text{pH} = 7.4$
$[\text{Pi}]_\text{tot} = 0\text{mM}$
$[\text{MgADP}] = 0\text{mM}$
$T = 297\text{K}$

Figure 3: Fit of the updated Terkildsen model to metabolite dependence data. Simulation conditions are displayed on the right of each figure. **(a)** Comparison of model to intracellular sodium data (Hansen et al., 2002, Fig. 7(a)), normalised to the cycling velocity at $[\text{Na}]_\text{i} = 50\text{mM}$. **(b)** Comparison of model to extracellular potassium data (Nakao and Gadsby, 1989, Fig. 11(a)), normalised to the cycling velocity at $[\text{K}]_\text{e} = 5.4\text{mM}$. **(c)** Comparison of model to ATP data (Friedrich et al., 1996, Fig. 3(b)), normalised to the cycling velocity at $[\text{MgATP}] = 0.6\text{mM}$.

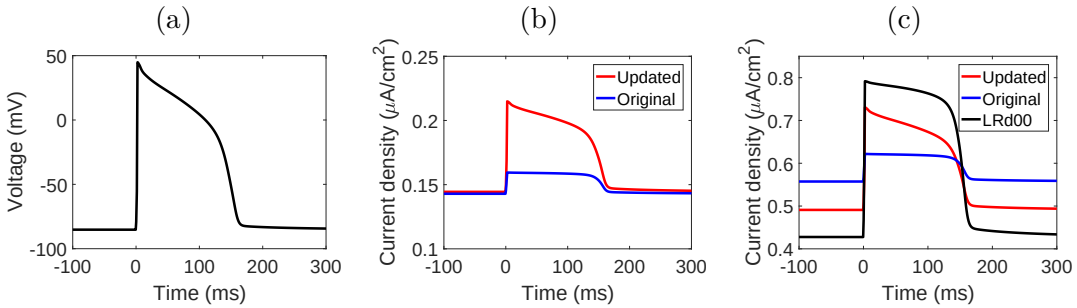

Figure 4: A comparison of the updated Terkildsen model to existing models. (a) The action potential waveform used to simulate the pumps (Faber and Rudy, 2000); (b) The Na^+/K^+ ATPase currents of the original and updated models; (c) A comparison of scaled versions of the updated and original models against the Na^+/K^+ ATPase model in Faber and Rudy (2000). The pump density was increased by a factor of 3.4 in the updated model, and by a factor of 3.9 in the original model. $[Na^+]_i = 10$mM, $[Na^+]_e = 140$mM, $[K^+]_i = 145$mM, $[K^+]_e = 5.4$mM, pH $= 7.095$, $[Pi]_{tot} = 0.8$mM, [MgATP] $= 6.95$mM, [MgADP] $= 0.035$mM, $T = 310$K.

The response of the updated model to an action potential input was simulated by using an action potential waveform generated from the Luo and Rudy 2000 (LRd00) model (Faber and Rudy, 2000; Luo and Rudy, 1994) (Figure 4(a)). A comparison of the response between the updated model and the original model is shown in Figure 4(b). The two models behave almost identically at resting membrane potentials, but the updated model has a much higher current during the action potential. As noted in Terkildsen (2006), the current of the pump is far lower at physiological intracellular sodium concentrations, thus the pump density needs to be appropriately scaled to be compatible with the LRd00 model. We compared scaled versions of the updated and original models to the Na^+/K^+ ATPase current described using equations in the LRd00 model and found that both versions of the Terkildsen et al. model exhibit similar behaviour to the description in the LRd00 model (Figure 4(c)). The updated model behaves more closely to the LRd00 Na^+/K^+ ATPase model because it has a more variable current. Thus we hypothesise that under physiological concentrations, the updated model has better compatibility with the LRd00 whole-cell model. A CellML version of the updated model is included with this paper, and reproduces the curve for $[Na]_e = 150$mM in Figure 2(a).

4 Bond graph model

To verify the physical plausibility of the updated model, and to aid its incorporation into larger models, we developed a bond graph version of the updated model. The bond graph model represents the full unsimplified biochemical cycle, and reactions that were assumed to be in rapid equilibrium were replaced by reactions with fast kinetic parameters with the same equilibrium constant. The structure of the bond graph is given in Figure 6 of Appendix B. We find the parameters of the bond graph model (Gawthrop et al., 2015) by solving the matrix equation

$$\mathbf{Ln}(\mathbf{k}) = \mathbf{MLn}(\mathbf{W}\boldsymbol{\lambda}) \tag{10}$$

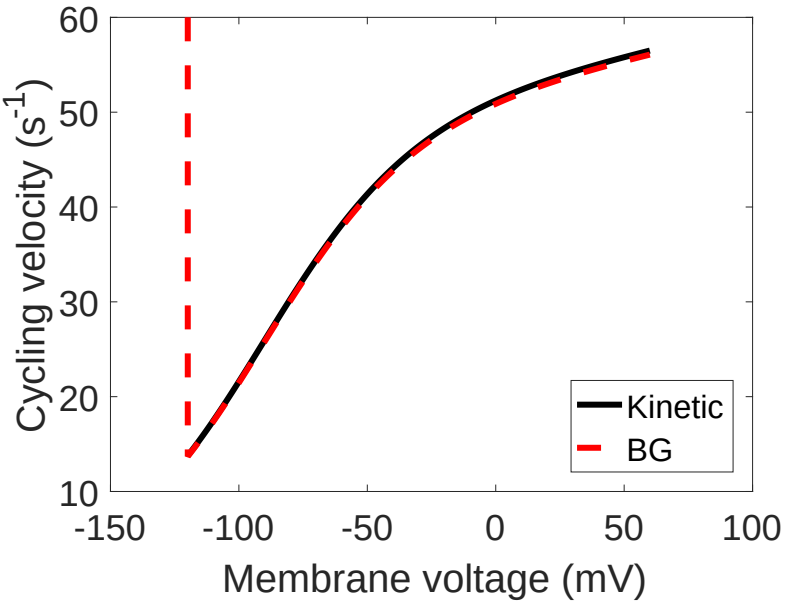

Figure 5: A comparison of the kinetic and bond graph models. $[Na^+]_i = 50mM$, $[Na^+]_e = 150mM$, $[K^+]_i = 0mM$, $[K^+]_e = 5.4mM$, pH = 7.4, $[Pi]_{tot} = 0mM$, [MgATP] = 10mM, [MgADP] = 0mM, $T = 310K$. In the bond graph model, zero concentrations were approximated by using a concentration of 0.001mM to avoid undefined values.

where **Ln** is the element-wise logarithm operator and

$$\mathbf{k} = \begin{bmatrix} k^+ \\ k^- \\ k^c \end{bmatrix}, \quad \mathbf{M} = \left[\begin{array}{c|c} I_{n_r \times n_r} & N^{f^T} \\ \hline I_{n_r \times n_r} & N^{r^T} \\ \hline 0 & N^c \end{array}\right], \quad \boldsymbol{\lambda} = \begin{bmatrix} \kappa \\ K \end{bmatrix} \tag{11}$$

We define the partitions of $\mathbf{k}$, $\boldsymbol{\lambda}$ and $\mathbf{M}$ as

$$k^+ = \text{column vector of forward rate constants} \tag{12}$$
$$k^- = \text{column vector of reverse rate constants} \tag{13}$$
$$\kappa = \text{column vector of reaction rate constants} \tag{14}$$
$$K = \text{column vector of species thermodynamic constants} \tag{15}$$
$$N^f = \text{forward stoichiometric matrix} \tag{16}$$
$$N^r = \text{reverse stoichiometric matrix} \tag{17}$$

The matrices k^c and N^c were used to enforce further constraints between species thermodynamic constants. These constraints describe the equilibria of the identical ions in different compartments, and the equilibrium constant of ATP hydrolysis. Assuming that equation (10) can be solved, one possible solution is given by

$$\boldsymbol{\lambda_0} = \mathbf{W}^{-1}\mathbf{Exp}(\mathbf{M}^\dagger \mathbf{Ln}(\mathbf{k})) \tag{18}$$

where **Exp** is the element-wise exponential operator and $\mathbf{M}^\dagger$ is the Moore-Penrose pseudoinverse of $\mathbf{M}$. For this bond graph model, we use the diagonal matrix $\mathbf{W}$ to scale the species thermodynamic constants according to the volume they reside in. For consistency with Terkildsen et al. (2007), an intracellular volume of $W_i = 38pL$ was

used for the species Na_i^+, K_i^+, MgATP, MgADP, Pi and H^+, an extracellular volume of $W_e = 5.182$pL was used for Na_e^+, K_e^+, and a constant of 1 was used for each of the pump states.

The bond graph model was simulated under the conditions described in Figure 2(a) to reproduce the curve for $[Na]_e = 150$mM. The membrane voltage was increased at a slow rate to induce quasi-steady-state behaviour. There is a high degree of correspondence between the kinetic and bond graph models (Figure 5). The only substantial difference occurs near the initial voltage of $V = -120$mV, where the bond graph model moves towards its steady state. The CellML code describing the bond graph model is provided with this paper, and reproduces the curve in Figure 5.

5 Conclusion

In this paper, we updated the Na^+/K^+ ATPase model by Terkildsen et al. (2007) to make it reproducible and thermodynamically consistent. We found errors in the analysis in the original paper which resulted in inaccurate descriptions of pump kinetics and ultimately a thermodynamically inconsistent model. Thus the equations and constraints within the model were corrected to make it thermodynamically consistent. We refitted the updated model to data, and simulations matched experimental measurements well. Since the updated model is thermodynamically consistent, it has a natural bond graph representation. We developed a bond graph version of the model to demonstrate thermodynamic consistency. CellML and MATLAB code for both the kinetic and bond graph models have been included with this paper to aid reproducibility. The thermodynamic consistency and reusability of our updated model make it ideal for incorporation into future whole-cell models to study cardiac cell energetics.

References

Apell, H.J., 1989. Electrogenic properties of the Na,K pump. The Journal of Membrane Biology 110, 103–114.

Borutzky, W., 2010. Bond Graph Methodology. Springer.

Faber, G.M., Rudy, Y., 2000. Action Potential and Contractility Changes in $[Na+]_i$ Overloaded Cardiac Myocytes: A Simulation Study. Biophysical Journal 78, 2392–2404.

Friedrich, T., Bamberg, E., Nagel, G., 1996. Na^+,K^+-ATPase pump currents in giant excised patches activated by an ATP concentration jump. Biophysical Journal 71, 2486–2500.

Gawthrop, P., Bevan, G., 2007. Bond-graph modeling. IEEE Control Systems 27, 24–45.

Gawthrop, P., Smith, L., 1996. Metamodelling: for bond graphs and dynamic systems. Prentice Hall international series in systems and control engineering, Prentice Hall, London, New York.

Gawthrop, P.J., Crampin, E.J., 2014. Energy-based analysis of biochemical cycles using bond graphs. Proceedings of the Royal Society of London A: Mathematical, Physical and Engineering Sciences 470, 20140459.

Gawthrop, P.J., Cursons, J., Crampin, E.J., 2015. Hierarchical bond graph modelling of biochemical networks. Proc. R. Soc. A 471, 20150642.

Guynn, R.W., Veech, R.L., 1973. The Equilibrium Constants of the Adenosine Triphosphate Hydrolysis and the Adenosine Triphosphate-Citrate Lyase Reactions. Journal of Biological Chemistry 248, 6966–6972.

Hansen, P.S., Buhagiar, K.A., Kong, B.Y., Clarke, R.J., Gray, D.F., Rasmussen, H.H., 2002. Dependence of Na^+-K^+ pump current-voltage relationship on intracellular Na^+, K^+, and Cs^+ in rabbit cardiac myocytes. American Journal of Physiology - Cell Physiology 283, C1511–C1521.

Keener, J., Sneyd, J., 2009. Mathematical Physiology. volume 8/1 of *Interdisciplinary Applied*

Mathematics. Springer New York, New York, NY.

Kennedy, J., Eberhart, R., 1995. Particle swarm optimization, in: IEEE International Conference on Neural Networks, 1995. Proceedings, pp. 1942–1948 vol.4.

Lloyd, C.M., Halstead, M.D.B., Nielsen, P.F., 2004. CellML: its future, present and past. Progress in Biophysics and Molecular Biology 85, 433–450.

Luo, C.H., Rudy, Y., 1994. A dynamic model of the cardiac ventricular action potential. I. Simulations of ionic currents and concentration changes. Circulation Research 74, 1071–1096.

Nakao, M., Gadsby, D.C., 1989. [Na] and [K] dependence of the Na/K pump current-voltage relationship in guinea pig ventricular myocytes. The Journal of General Physiology 94, 539–565.

Oster, G., Perelson, A., Katchalsky, A., 1971. Network thermodynamics. Nature 234, 393–399.

Smith, N.P., Crampin, E.J., 2004. Development of models of active ion transport for whole-cell modelling: cardiac sodium–potassium pump as a case study. Progress in Biophysics and Molecular Biology 85, 387–405.

Terkildsen, J., 2006. Modelling Extracellular Potassium Accumulation in Cardiac Ischaemia. Masters Thesis. The University of Auckland.

Terkildsen, J.R., Crampin, E.J., Smith, N.P., 2007. The balance between inactivation and activation of the Na^+-K^+ pump underlies the triphasic accumulation of extracellular K^+ during myocardial ischemia. American Journal of Physiology - Heart and Circulatory Physiology 293, H3036–H3045.

Tran, K., Smith, N.P., Loiselle, D.S., Crampin, E.J., 2009. A Thermodynamic Model of the Cardiac Sarcoplasmic/Endoplasmic Ca^{2+} (SERCA) Pump. Biophysical Journal 96, 2029–2042.

A Parameters

Table 1: Kinetic parameters for the updated Terkildsen et al. model. Refer to Figure 1 for a schematic.

Parameter	Description	Value
k_1^+	Forward rate constant of reaction R6	1423.2 s^{-1}
k_1^-	Reverse rate constant of reaction R6	225.9048 s^{-1}
k_2^+	Forward rate constant of reaction R7	11564.8064 s^{-1}
k_2^-	Reverse rate constant of reaction R7	36355.3201 s^{-1}
k_3^+	Forward rate constant of reaction R13	194.4506 s^{-1}
k_3^-	Reverse rate constant of reaction R13	281037.2758 $mM^{-2}s^{-1}$
k_4^+	Forward rate constant of reaction R15	30629.8836 s^{-1}
k_4^-	Reverse rate constant of reaction R15	1.574×10^6 s^{-1}
$K^0_{\mathrm{d,Nai}}$	Voltage-dependent dissociation constant of intracellular Na^+	579.7295 mM
$K^0_{\mathrm{d,Nae}}$	Voltage-dependent dissociation constant of extracellular Na^+	0.034879 mM
$K_{\mathrm{d,Nai}}$	Voltage-independent dissociation constant of intracellular Na^+	5.6399 mM
$K_{\mathrm{d,Nae}}$	Voltage-independent dissociation constant of extracellular Na^+	10616.9377 mM
$K_{\mathrm{d,Ki}}$	Dissociation constant of intracellular K^+	16794.976 mM
$K_{\mathrm{d,Ke}}$	Dissociation constant of extracellular K^+	1.0817 mM
$K_{\mathrm{d,MgATP}}$	Dissociation constant of MgATP	140.3709 mM
Δ	Charge translocated by reaction R5	-0.0550
Pump density	Number of pumps per μm^2	1360.2624 μm^{-2}

Table 2: Parameters for the bond graph version of the updated Terkildsen et al. model. Parameters were derived by using an intracellular volume of 38pL and an extracellular volume of 5.182pL. Refer to Figure 6 for the bond graph schematic.

Component	Description	Parameter	Value
R1	Reaction R1	κ_1	330.5462 fmol/s
R2	Reaction R2	κ_2	132850.9145 fmol/s
R3	Reaction R3	κ_3	200356.0223 fmol/s
R4	Reaction R4	κ_4	2238785.3951 fmol/s
R5	Reaction R5	κ_5	10787.9052 fmol/s
R6	Reaction R6	κ_6	15.3533 fmol/s
R7	Reaction R7	κ_7	2.3822 fmol/s
R8	Reaction R8	κ_8	2.2855 fmol/s
R9	Reaction R9	κ_9	1540.1349 fmol/s
R10	Reaction R10	κ_{10}	259461.6507 fmol/s
R11	Reaction R11	κ_{11}	172042.3334 fmol/s
R12	Reaction R12	κ_{12}	6646440.3909 fmol/s
R13	Reaction R13	κ_{13}	597.4136 fmol/s
R14	Reaction R14	κ_{14}	70.9823 fmol/s
R15	Reaction R15	κ_{15}	0.015489 fmol/s
P_1	Pump state ATP–E_i K_2	K_1	101619537.2009 fmol^{-1}
P_2	Pump state ATP–E_i K_1	K_2	63209.8623 fmol^{-1}
P_3	Pump state ATP–E_i	K_3	157.2724 fmol^{-1}
P_4	Pump state ATP–E_i Na_1	K_4	14.0748 fmol^{-1}
P_5	Pump state ATP–E_i Na_2	K_5	5.0384 fmol^{-1}
P_6	Pump state ATP–E_i Na_3	K_6	92.6964 fmol^{-1}
P_7	Pump state P–E_i (Na_3)	K_7	4854.5924 fmol^{-1}
P_8	Pump state P–E_e Na_3	K_8	15260.9786 fmol^{-1}
P_9	Pump state P–E_e Na_2	K_9	13787022.8009 fmol^{-1}
P_{10}	Pump state P–E_e Na_1	K_{10}	20459.5509 fmol^{-1}
P_{11}	Pump state P–E_e	K_{11}	121.4456 fmol^{-1}
P_{12}	Pump state P–E_e K_1	K_{12}	3.1436 fmol^{-1}
P_{13}	Pump state P–E_e K_2	K_{13}	0.32549 fmol^{-1}
P_{14}	Pump state E_e (K_2)	K_{14}	156.3283 fmol^{-1}
P_{15}	Pump state ATP–Ee (K_2)	K_{15}	1977546.8577 fmol^{-1}
Ki	Intracellular K_i^+	K_{Ki}	0.0012595 fmol^{-1}
Ke	Extracellular K_e^+	K_{Ke}	0.009236 fmol^{-1}
Nai	Intracellular Na_i^+	K_{Nai}	0.00083514 fmol^{-1}
Nae	Extracellular Na_e^+	K_{Nae}	0.0061242 fmol^{-1}
MgATP	Intracellular MgATP	K_{MgATP}	2.3715 fmol^{-1}
MgADP	Intracellular MgADP	K_{MgADP}	7.976×10^{-5} fmol^{-1}
P_i	Free inorganic phosphate	K_{Pi}	0.04565 fmol^{-1}
H	Intracellular H^+	K_{H}	0.04565 fmol^{-1}
mem	Membrane capacitance	C_m	153400 fF
zF_5	Charge translocated by R5	z_5	−0.0550
zF_8	Charge translocated by R8	z_8	−0.9450

B Bond graph model structure

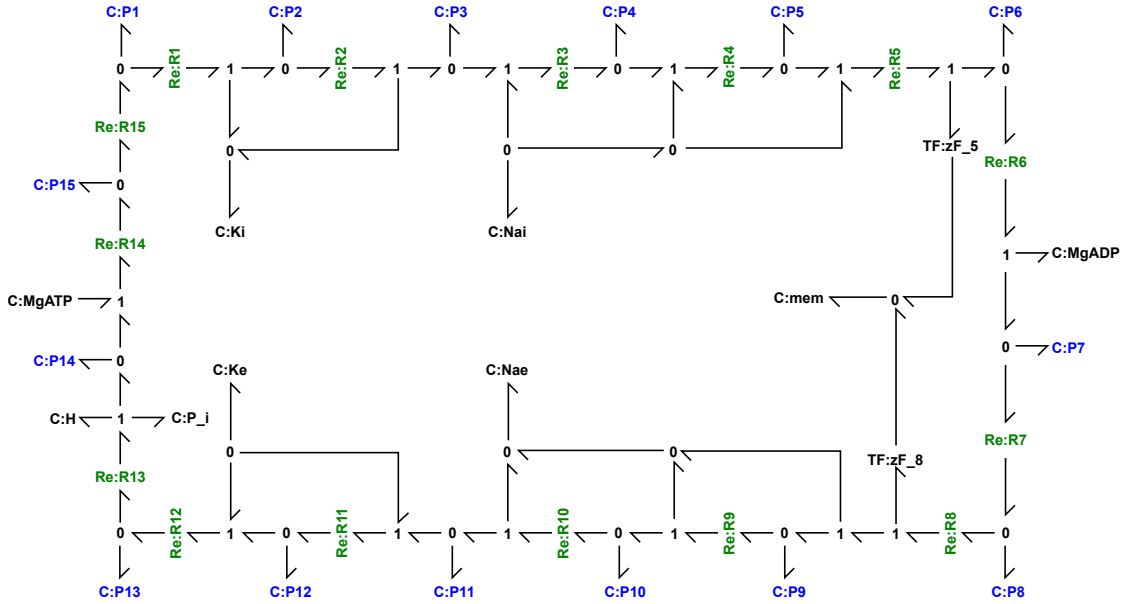

Figure 6: Bond graph structure of the Terkildsen et al. model. Pump states are coloured in blue, and reactions are coloured in green. The names for these components are consistent with their labels in Figure 1.